

## A New Method of Analyzing the Dispersion of Oceanic Rayleigh Waves

J. C. SAVAGE

*Geophysics Laboratory, University of Toronto  
Toronto 5, Ontario, Canada*

For the period range from about 25 sec to perhaps 80 sec, the group velocity  $U$  for oceanic Rayleigh waves may be approximated as a function of frequency  $f$  by  $1/U = 1/U_0 + B(f - f_0)^2$ . The subscript 0 refers to the group velocity maximum. A simple method of analyzing the Airy phase to obtain the constants  $U_0$ ,  $B$ , and  $f_0$  is shown. The fit is easily checked by calculating a synthetic seismogram to be compared with the original. In a study of 18 Rayleigh wave trains that had traversed different parts of the Pacific basin, the following ranges of values were found:  $U_0$ , 3.88–4.12 km/sec;  $T_0$  ( $=1/f_0$ ), 26.8–43.1 sec; and  $B$ , 24–107 sec<sup>3</sup>/km.

### INTRODUCTION

It is well known that the group velocity for oceanic Rayleigh waves reaches a maximum value usually somewhere in the period range 30 to 40 sec. The presence of this extremum makes the usual procedure for measuring the dispersion in wave trains difficult (see *Kuo et al.* [1962] for a brief description of this procedure), and the validity of the procedure becomes subject to question on theoretical grounds. *Kovach and Press* [1961] have shown empirically that the procedures are valid for the low frequency branch, and the consistency of the results of *Kuo et al.* [1962] for the long period branch leaves little doubt that the method is satisfactory there also. Thus, the new procedure proposed here is not intended to challenge the validity of the earlier results. Rather, it is proposed because it appears to be a more convenient procedure, and because it leads to an empirical formula for the dispersion of oceanic Rayleigh waves that appears to be of considerable value. Specifically, it is found that the group velocity  $U$  of oceanic Rayleigh waves can be represented by

$$1/U = 1/U_0 + B(f - f_0)^2$$

over a substantial range of frequency  $f$ . The values of the constants  $U_0$ ,  $B$ , and  $f_0$  are readily determined from a simple analysis of the Airy phase of the oceanic Rayleigh train.

### THEORY

It will suffice here to consider wave propagation in one dimension only (see *Knopoff and Schwab* [1968] for the modifications required to extend the theory to a wave spreading in two dimensions). We may represent the Rayleigh wave by a Fourier integral

$$y = \frac{1}{2\pi} \int_{-\infty}^{+\infty} \phi(\omega) \exp \{i\Theta(\omega, x, t)\} d\omega \quad (1)$$

where  $\phi(\omega)$  is the amplitude spectrum of the source and

$$\Theta(\omega, x, t) = \omega t - k(\omega)x + \vartheta(\omega) \quad (2)$$

The term  $\vartheta(\omega)$  represents the original phase spectrum of the source; it may, however, include other factors such as the phase shift introduced in recording the signal.

*Eckart* [1948] has shown how (1) may be approximated at times near the beginning of the Rayleigh phase. This first-arriving portion of the Rayleigh train, the so-called Airy phase, contains all of the important information we require. *Eckart's* procedure is to expand  $\Theta(\omega, x, t)$  in a Taylor series about the point  $\omega_0$

$$\begin{aligned} \Theta(\omega, x, t) = & \Theta(\omega_0, x, t) \\ & + \Theta'(\omega_0, x, t)(\omega - \omega_0) \\ & + \Theta''(\omega_0, x, t)(\omega - \omega_0)^2/2 \\ & + \Theta'''(\omega_0, x, t)(\omega - \omega_0)^3/6 + \dots \end{aligned} \quad (3)$$

where

$$\begin{aligned} \Theta' &= t - k'(\omega)x + \vartheta'(\omega) \\ &= t - x/U + \vartheta'(\omega) \end{aligned} \quad (4)$$

$$\begin{aligned} \Theta'' &= -k''(\omega)x + \vartheta''(\omega) \\ &= -x \frac{d}{d\omega} \left( \frac{1}{U} \right) + \vartheta''(\omega) \end{aligned} \quad (5)$$

$$\begin{aligned} \Theta''' &= -k'''(\omega)x + \vartheta'''(\omega) \\ &= -x \frac{d^2}{d\omega^2} \left( \frac{1}{U} \right) + \vartheta'''(\omega) \end{aligned} \quad (6)$$

The definition of the group velocity,  $U = d\omega/dk$ , has been used. The derivatives of  $\vartheta(\omega)$  will generally be small and can be neglected in the expressions above. (In fact, those terms may always be neglected asymptotically as  $x$  becomes large.) If  $\omega_0$  is chosen to coincide with the angular frequency at which  $U$  is a maximum, then  $\Theta''$  will be negligible. Furthermore, *Eckart* [1948] has shown that this choice is the appropriate one to describe the early portions of dispersed wave. If  $\phi(\omega)$  is a slowly varying function of  $\omega$ , then (1) may be approximated by

$$y \sim \phi(\omega_0) \exp \{ i\Theta(\omega_0, x, t) \} \cdot \frac{1}{2\pi} \int_{-\infty}^{+\infty} \exp \{ iz + i(\epsilon z)^3/3 \} dz \quad (7)$$

where

$$\begin{aligned} z &= \omega - \omega_0 \\ \tau &= \Theta'(\omega_0, x, t) = t - x/U(\omega_0) \end{aligned} \quad (8)$$

$$\epsilon^3 = \frac{1}{2} \Theta'''(\omega_0, x, t) = -\frac{x}{2} \left[ \frac{d^2}{d\omega^2} \left( \frac{1}{U} \right) \right]_{\omega=\omega_0} \quad (9)$$

The integral in (7) may be reduced to an Airy function

$$Ai(x) = \frac{1}{\pi} \int_0^{\infty} \cos(xt + t^3/3) dt$$

(see *Müller* [1946] for a brief review of the properties of this function and also a tabulation of its values) so that

$$y \sim [\phi(\omega_0)/\epsilon] \exp \{ i\Theta(\omega_0, x, t) \} Ai(\tau/\epsilon) \quad (10)$$

It is, of course, understood that only the real part of (10) is significant; thus

$$y \sim (\phi(\omega_0)/\epsilon) \cos(\omega_0\tau + \gamma) Ai(\tau/\epsilon) \quad (11)$$

where

$$\gamma = \omega_0 x(1/U_0 - 1/c_0) + \vartheta(\omega_0) \quad (12)$$

and  $c_0 = \omega_0/k(\omega_0)$  is the phase velocity at  $\omega_0$ .

The analytic expression (11) shows that the Airy phase is represented by the product of two oscillating functions, one a cosine function of constant period and the other an Airy function. Figure 1 shows the Airy function, the cosine function, and the product of the two. The latter, of course, represents the Airy phase. The important point here is that the zeros of the Airy phase must correspond either to the regularly spaced zeros of the cosine function or the irregularly spaced zeros of the Airy function. The regularity of the former sequence makes it relatively easy to separate the two sequences.

The procedure for analyzing the Airy phase is best explained by referring to an example. The upper section of Figure 2 shows a tracing of the vertical component of the Airy phase of

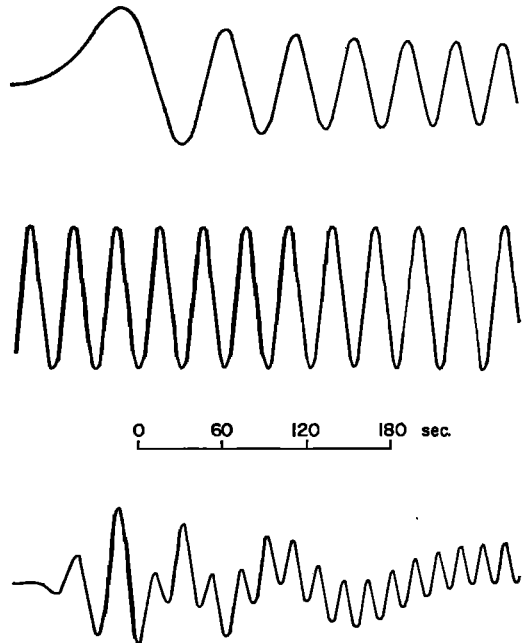


Fig. 1. A plot of the Airy function is shown at top, and a plot of a cosine function of constant period is shown in the center. The product of the two functions (shown in the bottom curve) represents the Airy phase.

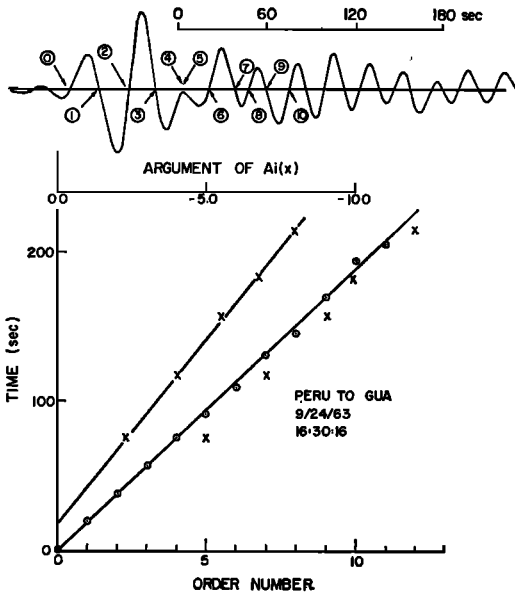


Fig. 2. A tracing of the Airy phase on a LPZ seismogram recorded at Guam from a shock at 16h 30m 16s GCT, September 24, 1963, near the coast of Peru is shown at the top. The lower figure shows the linear relation between the zeros of the cosine function (circles with dots) and the order number. The points (crosses) below the line identify points of zero displacement on the seismogram that do not fit the regular sequence established by the lower line. Those points have been replotted against the arguments at which the Airy function vanishes (upper line in lower figure). The linear relation that they exhibit in that plot confirms that those points represent zeros of the Airy function.

the Rayleigh wave as it arrived at Guam from an earthquake off the coast of Peru at 16h 30m 16s GCT September 24, 1963. First, draw a horizontal line through the seismogram to represent zero displacement of the trace. Then select one of the early crossings of the trace with this base line to serve as a local time origin. All time measurements will be made from this point. The arrow labeled 0 in Figure 2 indicates the local time origin chosen. Next, record the times of subsequent zero crossings out to a time 3 or 4 min beyond the local time origin, and assign an order number to each such crossing. (Order number 0 is given to the local time origin, and subsequent crossings are given numbers 1, 2, 3 . . .) The first 10 such crossings have been labeled in Figure 2. Notice that, if a maximum in the trace occurs below the base line, or if a

minimum occurs in the trace above the base line, it is usually necessary to assume that the base line is displaced and that a double crossing should be assigned to that extremum. An example is shown in Figure 2 where crossings 4 and 5 have been assigned to a maximum that actually lies below the base line. Now, plot the time of crossing against the order number for the first 4 or 5 points. Notice that these points closely define a straight line (Figure 2). Continue plotting points until one obviously deviates from the straight line defined by the preceding points. (In Figure 2, point with order number 5 clearly deviates from the line and for this reason it is plotted with a cross rather than a circled dot. That point must correspond to a zero of the Airy function and should be removed from the sequence being plotted that, of course, corresponds to the zeros of the cosine function. Removal of this point from the sequence requires that the order numbers for the subsequent points must each be reduced by 1. Plotting then proceeds as before until a second anomalous point is encountered. This point is removed from the sequence, the order numbers of the subsequent points are each reduced by 1, and then plotting is resumed. This process is continued until all points have been considered. The acceptable points represent the zeros of the cosine function in (11), and the slope of the straight line that best fits those points in the time-versus-order number plot must be  $T_0/2$  where  $T_0$  is the period corresponding to  $\omega_0$ . The sequence of points that has been rejected in the preceding analysis must correspond to zeros of  $Ai(y)$ . Let  $y_i$  ( $i = 1, 2, 3 \dots$ ) denote the values of the argument of the Airy function at which the Airy function itself is zero. Then (8) requires that  $\tau_i/\epsilon = y_i$ . The zero of  $\tau$  occurs at a time  $t_0$  (not yet known) after the local time zero. Then on the time scale used for measuring the zero crossings, we have

$$t_i - t_0 = \epsilon y_i$$

Thus, if the times  $t_i$  of the zero crossings that were rejected in the earlier analysis are plotted against the zeros of the Airy function ( $-2.34, -4.09, -5.52, -6.79, -7.94$ , etc.) the points should be along a straight line of slope  $\epsilon$  (note  $\epsilon$  is intrinsically negative). Moreover, the time-axis intercept of this line must equal  $t_0$ . Both

lines, one fitting each sequence of zeros, have been drawn in Figure 2. The estimates (with standard deviation) obtained from least-squares fits to those lines are

$$T_0 = (37.6 \pm 0.4) \text{ sec}$$

$$\epsilon = -(24.6 \pm 0.7) \text{ sec}$$

$$t_0 = (19.0 \pm 4.) \text{ sec}$$

The phase constant  $\gamma$  may also be obtained from Figure 2. The phase of the cosine wave at order number 0 is  $-\pi/2$  since the crossing goes from  $-$  to  $+$ . The phase at  $\tau = 0$  is then

$$\gamma = -\pi/2 + 2\pi t_0/T_0$$

In general

$$\gamma = \pm\pi/2 + 2\pi t_0/T_0 \quad (13)$$

where the upper sign is chosen if the crossing at order number 0 goes from  $+$  to  $-$  as time increases, and the lower sign is chosen if it goes from  $-$  to  $+$ . For the example shown in Figure 2,  $\gamma = 1.63$  radians. All of the constants that appear in (11) have now been obtained except the amplitude factor  $\phi(\omega_0)$ , and that value is not required. Inasmuch as the Airy function is a tabulated function [Miller, 1946], it is not difficult to compute the shape of the Airy phase from (11) and compare this with the actual seismogram. Such a comparison has been made in Figure 3. Notice that the overall agreement is quite good over the entire section (about 6 min) reproduced.

A Taylor series expansion of the reciprocal

group velocity about  $\omega_0$  yields

$$\frac{1}{U} = \frac{1}{U_0} + \left[ \frac{d^2}{d\omega^2} \left( \frac{1}{U} \right) \right]_{\omega=\omega_0} \cdot (\omega - \omega_0)^2 + \dots \quad (14)$$

In reducing the integral in (1) to an Airy function in (10), all terms of order  $(\omega - \omega_0)^3$  or higher in (14) were neglected. Thus, the procedure used in analyzing the Rayleigh wave is valid only insofar as the higher order terms in (14) are negligible. The fact that there is good agreement between the synthetic seismogram calculated from (11) and the observed seismogram over a time interval in excess of 5 min (see Figure 3) suggests that an adequate approximation to  $U$  over a broad frequency range is given by the first two terms in (14). Thus, an acceptable approximation is

$$1/U = 1/U_0 + B(f - f_0)^2 \quad (15)$$

where (from (9))

$$B = -4\pi\epsilon^3/x \quad (16)$$

and  $f = \omega/2\pi$  is the frequency. The constant  $U_0$  (the maximum group velocity) is readily calculated from (8) if the epicentral distance and origin time of the event that produced the Airy phase are known. Thus,  $U_0 = x/t$  where  $t$  is the interval between the origin time of the event and the time at which  $\tau = 0$  (i.e., the time corresponding to the local time origin plus  $t_0$ ). It might be noted that the definition of the group velocity ( $U = d\omega/dk$ ) implies that

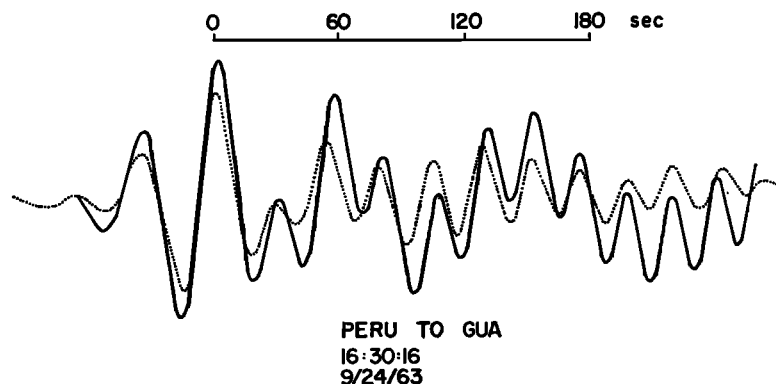


Fig. 3. Comparison of actual LPZ seismogram (dotted line) recorded at Guam and synthetic seismogram (solid line) computed for the Airy phase for the shock at 16h 30m 10s GCT September 24, 1963, located off the coast of Peru.

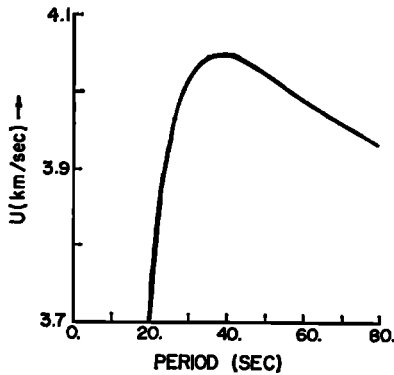


Fig. 4. Group velocity as a function of period for the great circle path from near the coast of Peru to Guam.

$k = \int d\omega/U$ . The phase velocity ( $c = \omega/k$ ), calculated from (15), is then found to be

$$1/c = 1/U_0 + (1/c_0 - 1/U_0) \cdot (f_0/f) + B(f - f_0)^3/(3f) \quad (17)$$

Unfortunately, the value of  $(1/c_0 - 1/U_0)$  is not known, although it could be determined from (12) if  $\vartheta(\omega_0)$  were known. It is very unlikely, however, that accurate estimates of  $\theta(\omega_0)$  will be available. For this reason there does not appear to be any reliable method of estimating  $c_0$  in this scheme. The work of *Kuo et al.* [1962] indicates the parameter  $(1/c_0 - 1/U_0)$  is quite small, probably much less than 0.005 sec/km.

The final result of the analysis of the Airy phase of Figure 2 is the group-velocity plot shown in Figure 4. The curve is a plot of (15) with the constants  $U_0 = 4.05$  km/sec,  $B = 37.9$  sec<sup>3</sup>/km, and  $T_0 = 37.6$  sec; and the curve represents the average value of the group velocity along the great circle path from the coast of Peru to Guam. The result appears to be consistent with other determinations for similar paths (see, for example, *Kuo et al.* [1962]).

The procedure employed here is the correct asymptotic treatment of the Airy phase. The important question, however, concerns the range of periods over which (15) is a valid approximation. We first consider the validity of the approximation on the short-period branch of the dispersion curve. Figure 3 shows that the short-period component of the synthetic seis-

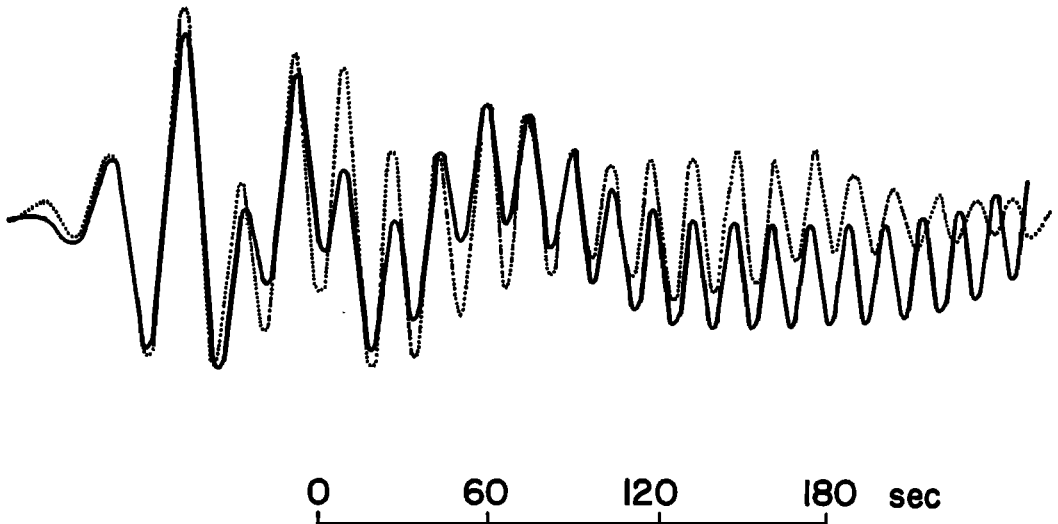
mogram agrees very well with the short-period component of the actual seismogram for an interval of almost 5 min following the arrival of the Airy phase. The group velocity of waves arriving 5 min after the arrival of the Airy phase is readily found from  $x/(t + 300)$  where  $x$  is the epicentral distance and  $t$  is the travel time in seconds for the period of maximum group velocity. Thus, the apparent group velocity of the late arriving periods is about 3.75 km/sec. Then, on the basis of the agreement observed in Figure 3, it would be expected that the approximations are valid at least down to that group velocity, which from Figure 4 appears to correspond to a period of about 20 sec. The limit of validity of the approximation on the long-period branch is more difficult to estimate. It certainly appears that the long-period components of the synthetic and actual seismograms in Figure 3 agree quite well for at least 2 min following the arrival of the Airy phase. This agreement would imply that the long-period branch is valid at least out to a group velocity of about 3.9 km/sec. From Figure 4 this implies that the approximation is valid to a period somewhat greater than 80 sec. Inasmuch as the true Rayleigh wave group velocity has minima at about 12 and also at about 225 sec, the quadratic approximation (15) will tend to give group velocities that are too low at both long and short periods. The range over which the approximation (15) is valid is difficult to estimate, but it appears that it probably extends from 20 to 80 sec. The overall consistency of these results with those of *Kuo et al.* [1962] supports this conclusion. It should be pointed out, however, that there is appreciable uncertainty in the results of *Kuo et al.* [1962] for the long-period branch. The method of stationary phase employed by those authors is not strictly applicable to a train of poorly dispersed waves such as the long-period Rayleigh waves following the Airy phase [see *Eckart*, 1948]. Moreover, the method employed by *Kuo et al.* [1962, p. 338] to filter out the short-period waves so that the long-period branch could be analyzed is clearly not very precise.

Figure 5 shows the comparison of two other seismograms with the synthetic Airy phases calculated to fit those records. It should be recalled in comparing the records that, in calculating

the synthetic seismogram, it has been assumed that the source spectrum (both  $\phi(\omega)$  and  $\vartheta(\omega)$ ) does not vary with frequency. This, of course, is not true, and appreciable deviations from the observed form must be expected. A clear example of a variation in  $\phi(\omega)$  is shown in the lower seismogram in Figure 5 where the short-period coda in the observed seismogram is

almost completely absent. Presumably, the short-period waves have been removed by absorption since the Palomar recording of the same shock shows a well-developed short-period coda (upper seismogram in Figure 7). To estimate the effects of a variation of  $\phi(\omega)$  with frequency, a synthetic Airy phase, calculated from (11), was numerically differentiated with re-

### EASTER ISLAND-PLM



### EASTER ISLAND-HNR

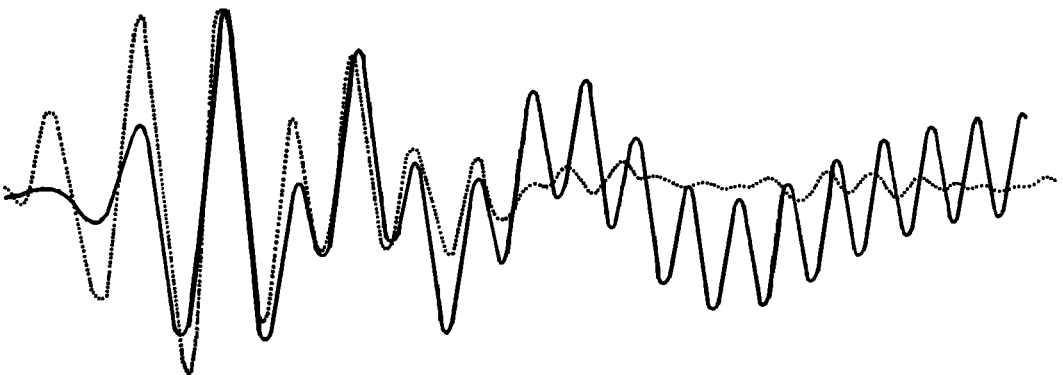


Fig. 5. Comparison of the actual LPZ seismograms (dotted lines) recorded at Palomar (upper) and Honiara (lower) with the synthetic seismograms (solid lines) computed for the Airy phase from the shock near Eastern Islands at 21h 09m 50.3s GCT, August 21, 1962.

TABLE 1. Earthquake Data for Rayleigh Wave Paths

Path No.	Date	Origin Time (GCT),			Lat., deg	Long., deg	Depth, km	Mag.	$\Delta$ , deg	Approximate Geographic Location	Recorded at
		h	m	s							
1	02/22/58	10	50	23	50.5 N	175 W	..	6.75	68.2	Andreanof Island	Suva
2	03/20/58	01	38	04	51 N	173 W	..	..	68.3	Fox Islands	Suva
3	03/22/60	02	31	17	61.5 S	154 E	..	..	46.4	Balleney Islands	Suva
4	08/21/62	21	09	50.3	29.6 S	111.9 W	33	6.5	83.8	Easter Island	HNR
5	08/21/62	21	09	50.3	29.6 S	111.9 W	33	6.5	94.8	Easter Island	PMG
6	08/21/62	21	09	50.3	29.6 S	111.9 W	33	6.5	62.8	Easter Island	PLM
7	08/21/62	21	09	50.3	29.6 S	111.9 W	33	6.5	93.1	Easter Island	RAB
8	09/24/63	16	30	16.0	10.6 S	78.0 W	80	6.75	91.1	Coast of Peru	AFI
9	09/24/63	16	30	16.0	10.6 S	78.0 W	80	6.75	138.0	Coast of Peru	GUA
10	09/24/63	16	30	16.0	10.6 S	78.0 W	80	6.75	119.0	Coast of Peru	HNR
11	11/15/63	21	06	34.0	44.3 N	149.0 E	50	6.25	68.0	Kuriles	AFI
12	11/15/63	21	06	34.0	44.3 N	149.0 E	50	6.25	30.8	Kuriles	GUA
13	11/15/63	21	06	34.0	44.3 N	149.0 E	50	6.25	54.4	Kuriles	HNR
14	11/15/63	21	06	34.0	44.3 N	149.0 E	50	6.25	48.4	Kuriles	RAB
15	02/23/65	22	11	50.2	25.7 S	70.5 W	80	7.0	93.9	Coast of Chile	AFI
16	02/23/65	22	11	50.2	25.7 S	70.5 W	80	7.0	144.7	Coast of Chile	GUA
17	02/23/65	22	11	50.2	25.7 S	70.5 W	80	7.0	119.8	Coast of Chile	HNR
18	07/02/65	20	58	40.0	53.1 N	167.7 W	59	6.75	66.8	Fox Islands	AFI
19	07/02/65	20	58	40.0	53.1 N	167.7 W	59	6.75	54.3	Fox Islands	GUA
20	07/02/65	20	58	40.0	53.1 N	167.7 W	59	6.75	68.1	Fox Islands	HNR
21	07/02/65	20	58	40.0	53.1 N	167.7 W	59	6.75	66.3	Fox Islands	RAB

spect to time to generate a second synthetic seismogram. The source amplitude spectrum for this second synthetic seismogram should be  $\omega\phi(\omega)$  rather than just  $\phi(\omega)$ . Both synthetic seismograms were then analyzed by the procedure described in this paper. No significant difference was found between the values of  $T_0$ ,  $U_0$ , and  $B$  calculated for the two cases. This suggests that the procedure is not particularly sensitive to changes in the source spectrum.

#### RESULTS

Twenty-one different Rayleigh wave trains, each of which had traversed a path within the Pacific basin, have been analyzed by the procedure described here. The pertinent information on these Rayleigh waves is given in Table 1. In three cases (events numbered 17, 18, and 19 in Table 1) the calculated synthetic seismogram was not very similar to the actual seismogram, although the calculated values of  $U_0$ ,  $T_0$ , and  $B$  appeared to be reasonably consistent with the other results. These three events were rejected, and the data presented here restricted to solutions that yielded satisfactory agreement between the calculated and observed seismograms. The results for the 18 successful cases

are shown in Table 2. The group-velocity curves for these paths are shown in Figure 6. The first three events in Table 1 were also among those events studied by *Kuo et al.* [1962]. The group-velocity curves for these 3 events are reasonably

TABLE 2. Dispersion Parameters

Path No.	$U_0$ , km/sec	$T_0$ , sec	$B$ , sec <sup>3</sup> /km
1	4.04 ± 0.05	39.7 ± 0.7	29.0 ± 2.0
2	4.07 ± 0.05	38.6 ± 0.5	48.0 ± 4.0
3	3.90 ± 0.06	32.0 ± 0.6	69.0 ± 3.0
4	3.88 ± 0.04	31.4 ± 0.4	33.0 ± 4.0
5	3.97 ± 0.04	35.9 ± 0.6	42.0 ± 3.0
6	3.90 ± 0.04	26.8 ± 0.3	24.0 ± 3.0
7	3.90 ± 0.03	36.1 ± 0.5	40.0 ± 2.0
8	4.01 ± 0.03	31.0 ± 0.3	24.0 ± 2.0
9	4.05 ± 0.03	37.6 ± 0.4	38.0 ± 3.0
10	4.03 ± 0.03	34.2 ± 0.1	67.0 ± 19.0
11	4.12 ± 0.05	38.4 ± 0.4	80.0 ± 5.0
12	3.89 ± 0.10	33.9 ± 0.5	107.0 ± 12.0
13	4.05 ± 0.07	41.6 ± 0.6	102.0 ± 10.0
14	4.07 ± 0.07	40.2 ± 0.5	69.0 ± 5.0
15	3.99 ± 0.03	28.3 ± 0.3	56.0 ± 7.0
16	4.03 ± 0.02	34.5 ± 0.4	39.0 ± 3.0
20	4.07 ± 0.06	43.1 ± 0.6	58.0 ± 8.0
21	4.03 ± 0.06	40.7 ± 0.7	32.0 ± 3.0

consistent with the results of *Kuo et al.* [1962]. The major discrepancy occurs for event 3 where the velocities for the long-period waves given by Figure 6 are almost certainly too low. This same conclusion is reached from an uncertainty estimate similar to that made for event 9. It would appear that the group-velocity curves for events 3, 12, and 15 probably should not be extended beyond 60-sec periods.

In Figure 6, the higher group of curves is typical of the deep oceanic basins, and the lower group is typical of the shallower parts of the ocean. The portion of the curves at periods less than about 25 sec is largely determined by the water depth along the path. Thus, the interesting part of the curves is the portion at periods longer than about 25 sec, and it is over that portion that the method described in this paper is most effective.

The curve representing path 12 (Kuriles to

Guam) is perhaps the most exceptional in Figure 6. A large proportion of this path lies along the oceanic trenches, and the trenches are known to be regions of anomalous crustal structure. Path 3 (Balleny Islands to Suva) is also anomalous, and the reason here appears to be that this path includes a large segment of the continent-like platform surrounding New Zealand. As already mentioned, it does not appear that the extension of either curve 3 or 12 to periods longer than about 60 sec is justified.

Paths 1, 2, and 3, representing seismograms analyzed by *Kuo et al.* [1962], were included partly to check the results of this analysis against the older method. The major reason for including these seismograms, however, was to test a hypothesis of *Cleary and Peaslee* [1962]. Those authors contended that these three seismograms exhibited effects of nonlinear interaction. The present method of analysis shows that

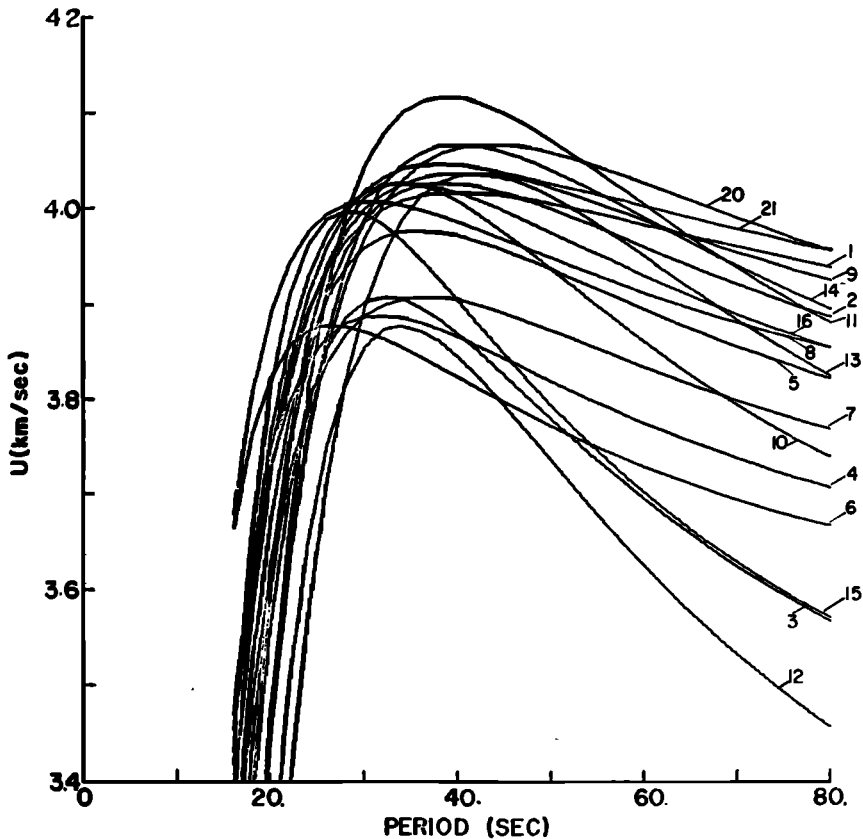


Fig. 6. Group velocity as a function of period found from the analysis of 18 different Airy phases. See Table 1 for identification of paths by number.

an adequate fit to the observed seismograms may be obtained without invoking nonlinear interactions. Figure 7 shows an example of the fit that can be obtained. It appears that the error in the reasoning of Cleary and Peaslee lies in the assumption that the Airy function is a non-oscillating function (see p. 4745 of their paper). In fact, the Airy function is a relatively rapidly oscillating function as may be seen in the upper part of Figure 1.

The preceding discussion has been concerned solely with the average dispersion along a great circle path from earthquake epicenter to recording station. Of greater physical significance would be knowledge of the local group-velocity curves at various points within the oceanic basins. The formulation of the group-velocity information in the form of (15) should facilitate such a solution. For example, the dispersion relation (15) for the *i*th oceanic path can be written in the form

$$1/U_i = G_i + E_i f + B_i f^2 \tag{18}$$

where *G* and *E* bear an obvious relation to the constants *U*<sub>0</sub>, *B*, and *f*<sub>0</sub> in (15). Assume that the local dispersion relation can be written in the same form

$$1/u = g + ef + bf^2 \tag{19}$$

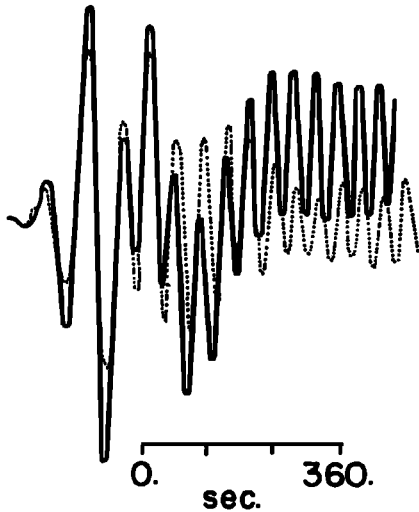


Fig. 7. Comparison of the actual LPZ seismogram (dotted line) recorded at Suva with the synthetic seismogram (solid line) computed for the Airy phase from the shock near Fox Islands at 01h 38m 04s GCT, March 20, 1958.

where *g*, *e*, and *b* are, of course, functions of the latitude and longitude. Inasmuch as *U<sub>i</sub>* is the average group velocity for the path

$$\Delta_i/U_i = \int d\Delta_i/u \tag{20}$$

where  $\Delta_i$  is the total length of the *i*th path and the integral on the right of (20) is along that path. From (18), (19), and (20), we have

$$\begin{aligned} G_i &= \Delta_i^{-1} \int g \, d\Delta_i \\ E_i &= \Delta_i^{-1} \int e \, d\Delta_i \\ B_i &= \Delta_i^{-1} \int b \, d\Delta_i \end{aligned} \tag{21}$$

Assume *g*, *e*, and *b* can be approximated by a series in the sequence of functions *Z<sub>i</sub>*, where each *Z<sub>i</sub>* is, of course, a function of both longitude and latitude (e.g., the functions *Z<sub>i</sub>* might be spherical surface harmonics). Then, since  $g = \sum \gamma_j Z_j$ , we have from (21)

$$G_i = \sum \gamma_j W_{ij} \tag{22}$$

where

$$W_{ij} = \Delta_i^{-1} \int Z_j \, d\Delta_i$$

The values of *W<sub>ij</sub>* are readily determined by direct integration. If there are *n* paths (i.e.,  $i \leq n$ ) and *m* coefficients (i.e.,  $j \leq m$ ) with  $n > m$ , the system of equations given by (22) may be solved for the  $\gamma_j$  by least squares. Similar solutions can be found for the coefficients in the expansions of *e* and *b*. Thus *g*, *e*, and *b* could be determined as functions of latitude and longitude. Equation 19 may be reduced to the form of (15) by setting

$$f_0 = -e/2b \tag{23}$$

$$u_0 = 1/(g - e^2/4b) \tag{24}$$

The results could be represented by contour maps of *u*<sub>0</sub> (the local maximum group velocity), *f*<sub>0</sub> (the frequency at the local group-velocity maximum) and *b* on a map of the oceanic basin. Data are now being accumulated to attempt this type of fit. A preliminary attempt with only the data of Table 2 has given encouraging results.

*Acknowledgment.* This research was supported by a grant from the National Research Council of Canada.

## REFERENCES

- Cleary, J. R., and D. C. Peaslee, Amplitude perturbations in Rayleigh waves, *J. Geophys. Res.*, *67*, 4741-4749, 1962.
- Eckart, C., The approximate solution of one-dimensional wave equations, *Rev. Mod. Phys.*, *20*, 399-417, 1948.
- Knopoff, L., and F. A. Schwab, Apparent initial phase of a source of Rayleigh waves, *J. Geophys. Res.*, *73*, 755-760, 1968.
- Kovach, R. L., and F. Press, Rayleigh wave dispersion and crustal structure in the Eastern Pacific and Indian Oceans, *Geophys. J.*, *4*, 202-216, 1961.
- Kuo, J., J. Brune, and M. Major, Rayleigh wave dispersion in the Pacific Ocean for the period range 20 to 140 seconds, *Bull. Seismol. Soc. Am.*, *52*, 333-357, 1962.
- Miller, J. C. P., *The Airy Integral (BAAS Math Tables Part-Volume B)*, Cambridge University Press, Cambridge, 1946.

(Received June 13, 1968.)